ProtNN: Fast and Accurate Nearest Neighbor Protein Function Prediction based on Graph Embedding in Structural and Topological Space

Wajdi Dhifli[1], and Abdoulaye Baniré Diallo [1,*]

[1] Department of Computer Science, University of Quebec At Montreal, PO box 8888, Downtown station, Montreal, Qc, Canada, H3C 3P8.

[*] To whom correspondence should be addressed.

Abstract

Motivation: Studying the function of proteins is important for understanding the molecular mechanisms of life. The number of publicly available protein structures has increasingly become extremely large. Still, the determination of the function of a protein structure remains a difficult, costly, and time consuming task. The difficulties are often due to the essential role of spatial and topological structures in the determination of protein functions in living cells.

Results: In this paper, we propose ProtNN, a novel approach for protein function prediction. Given an unannotated protein structure and a set of annotated proteins, ProtNN finds the nearest neighbor annotated structures based on protein-graph pairwise similarities. Given a query protein, ProtNN finds the nearest neighbor reference proteins based on a graph representation model and a pairwise similarity between vector embedding of both query and reference protein-graphs in structural and topological spaces. ProtNN assigns to the query protein the function with the highest number of votes across the set of k nearest neighbor reference proteins, where k is a user-defined parameter. Experimental evaluation demonstrates that ProtNN is able to accurately classify several datasets in an extremely fast runtime compared to state-of-the-art approaches. We further show that ProtNN is able to scale up to a whole PDB dataset in a single-process mode with no parallelization, with a gain of thousands order of magnitude of runtime compared to state-of-the-art approaches.

Availability: An implementation of ProtNN as well as the experimental datasets are available at https://sites.google.com/site/wajdidhifli/softwares/protnn.

Contact: diallo.abdoulaye@uqam.ca

1 Introduction

Proteins are ubiquitous in the living cells. They play key roles in the functional and evolutionary machinery of species. Studying protein functions is paramount for understanding the molecular mechanisms of life. High-throughput technologies are yielding millions of protein-encoding sequences that currently lack any functional characterization (Brenner and Levitt, 2000; Lee *et al.*, 2007; Molloy *et al.*, 2014) The number of proteins in the Protein Data Bank (PDB) (Berman *et al.*, 2000) has more than tripled over the last decade. Alternative databases such as SCOP (Andreeva *et al.*, 2008) and CATH (Sillitoe *et al.*, 2015) are undergoing the same trend. However, the determination of the function of protein structures remains a difficult, costly, and time consuming task. Manual protein functional classification methods are no longer able to follow the rapid increase of data. Accurate computational and machine learning tools present an efficient alternative that could offer considerable boosting to meet the increasing load of data.

Proteins are composed of complex three-dimensional folding of long chains of amino acids. This spatial structure is an essential component

in protein functionality and is thus subject to evolutionary pressures to optimize the inter-residue contacts that support it (Meysman *et al.*, 2015). Existing computational methods for protein function prediction try to simulate biological phenomena that define the function of a protein. The most conventional technique is to perform a similarity search between an unknown protein and a reference database of annotated proteins with known functions. The query protein is assigned with the same functional class of the most similar (based on the sequence or the structure) reference protein. There exists several classification methods based on the protein sequence (*e.g.* Blast (Altschul *et al.*, 1990), ...); or on the protein structure (*e.g.* Combinatorial Extension (Shindyalov and Bourne, 1998), Sheba (Jung and Lee, 2000), FatCat (Ye and Godzik, 2003), Fragbag (Budowski-Tal *et al.*, 2010), ...). These methods rely on the assumption that proteins sharing the most common sites are more likely to share functions. This classification strategy is based on the hypothesis that structurally similar proteins could share a common ancestor (Borgwardt *et al.*, 2005). Another popular approach for protein functional classification is to look for relevant substructures (also so-called motifs) among proteins with known functions, then use them as features to identify the function of unknown proteins. Such motifs could be discriminative (Zhu *et al.*, 2012), representative (Dhifli *et al.*,

2014), cohesive (Meysman *et al.*, 2015), *etc.* Each of the mentioned protein functional classification approaches suffers different drawbacks. Sequence-based classification do not incorporate spatial information of amino acids that are not contiguous in the primary structure but interconnected in 3D space. This makes them less efficient in predicting the function for structurally similar proteins with low sequence similarity (remote homologues). Both structure and substructure-based classification techniques do incorporate spatial information in function prediction which makes them more efficient than sequence-based classification. However, such consideration makes these methods subject to the *"no free lunch"* principle (Wolpert and Macready, 1997), where the gain in accuracy comes with an offset of computational cost. Hence, it is essential to find an efficient way to incorporate 3D-structure information with low computational complexity.

In this paper, we present ProtNN, a novel approach for function prediction of protein 3D-structures. ProtNN incorporates protein 3D-structure information via the combination of a rich set of structural and topological descriptors that guarantee an informative multi-view representation of the structure that considers spatial information through different dimensions. Such a representation transforms the complex protein 3D-structure into an attribute-vector of fixed size allowing computational efficiency. For classification, ProtNN assigns to a query protein the function with the highest number of votes across the set of its k most similar reference proteins, where k is a user-defined parameter. Experimental evaluation shows that ProtNN is able to accurately classify different benchmark datasets with a gain of up to 47x of computational cost compared to gold standard approaches from the literature such as Combinatorial Extension (Shindyalov and Bourne, 1998), Sheba (Jung and Lee, 2000), FatCat (Ye and Godzik, 2003) and others. We further show that ProtNN is able to scale up to a PDB-wide dataset in a single-process mode with no parallelization, where it outperformed state-of-the-art approaches with thousands order of magnitude in runtime on classifying a 3D-structure against the entire PDB.

2 Methods

2.1 Graph Representation of Protein 3D-Structures

A crucial step in computational studies of protein 3D-structures is to look for a convenient representation of their spatial conformations. Graphs represent the most appropriate data structures to model the complex structures of proteins. In this context, a protein 3D-structure can be seen as a set of elements (amino acids and atoms) that are interconnected through chemical interactions (Borgwardt *et al.*, 2005; Dhifli *et al.*, 2014; Meysman *et al.*, 2015). These interactions are mainly:

- Covalent bonds between atoms sharing pairs of valence electrons,
- Ionic bonds of electrostatic attractions between oppositely charged components,
- Hydrogen bonds between two partially negatively charged atoms sharing a partially positively charged hydrogen,
- Hydrophobic interactions where hydrophobic amino acids in the protein closely associate their side chains together,
- Van der Waals forces which represent transient and weak electrical attraction of one atom for another when electrons are fluctuating.

These chemical interactions are supposed to be the analogues of graph edges. Figure 1 shows a real example of the human hemoglobin protein and its graph representation. The Figure shows clearly that the graph representation preserves the overall structure of the protein and its components.

2.1.1 Protein Graph Model
Let G be a graph consisting of a set of nodes V and edges E. L is a label function that associates a label l to each node in V. Each node of G represents an amino acid from the 3D-structure, and is labeled with its corresponding amino acid type. Let Δ be a function that computes the euclidean distance between pairs of nodes $\Delta(u,v), \forall u,v \in V$, and δ a distance threshold. Each node in V is defined by its 3D coordinates in $\mathbb{R}^3$, and both Δ and δ are expressed in angstroms (). Two nodes u and v ($\forall u,v \in V$) are linked by an edge $e(u,v) \in E$, if the distance between their C_α atoms is below or equal to δ. Formally, the adjacency matrix A of G is defined as follows:

$$A_{u,v} = \begin{cases} 1, \ if \ \Delta(C_{\alpha_u}, C_{\alpha_v}) \leq \delta \\ 0, \ otherwise \end{cases} \tag{1}$$

2.2 Structural and Topological Embedding of Protein Graphs

2.2.1 Graph Embedding
Graph-based representations are broadly used in multiple application fields including bioinformatics (Borgwardt *et al.*, 2005; Gibert *et al.*, 2010; Dhifli *et al.*, 2014). However, they suffer major drawbacks with regards to processing tools and runtime. Graph embedding into vector spaces is a very popular technique to overcome both drawbacks (Gibert *et al.*, 2010). It aims at providing a feature vector representation for every graph, allowing to bridge the gap between the representational power of graphs, the rich set of algorithms that are available for feature-vector representations, and the need for rapid processing algorithms to handle the massively available biological data. In ProtNN, each protein 3D-structure is represented by a graph according to Equation 1. Then, each graph is embedded into a vector of structural and topological features under the assumption that structurally similar graphs should give similar structural and topological feature-vectors. In such manner, ProtNN guarantees accuracy and computational efficiency. It is worth noting that even though structurally similar graphs should have similar topological properties, ProtNN similarity should not necessarily give the same results of structure matching (as in structural alignment). But, it should enrich it since ProtNN considers even hidden similarities (like graph density and energy) that are not considered in structure matching.

2.2.2 Structural and Topological Attributes
In ProtNN, the pairwise similarity between two protein-graphs is measured by the distance between their vector representations. In order to avoid the loss of structural information in the embedding, and to guarantee ProtNN accuracy, we use a set of structural and topological attributes from the literature that have shown to be interesting and efficient in describing connected graphs (Leskovec *et al.*, 2005; Li *et al.*, 2012). It is important to mention that this list could be extended as needed. In the following is the list of structural and topological attributes used in ProtNN:

A1- **Number of nodes**: The total number of nodes of the graph, $|V|$.
A2- **Number of edges**: The total number of edges of the graph, $|E|$.
A3- **Average degree**: The degree of a node u, denoted $deg(u)$, is the number of its adjacent nodes. The average degree of a graph G is the average of all $deg(u)$, $\forall u \in G$. Formally: $deg(G) = \frac{1}{|V|} \sum_{i=1}^{|V|} deg(u_i)$.
A4- **Density**: The density of a graph $G = (V, E)$ measures how many edges are in E compared to the number of maximum possible edges between the nodes in V. Formally: $den(G) = \frac{2|E|}{(|V|*(|V|-1))}$.
A5- **Average clustering coefficient**: The clustering coefficient of a node u, denoted $c(u)$, measures how complete the neighborhood of u is, $c(u) = \frac{2e_u}{k_u(k_u-1)}$ where k_u is the number of neighbors of u and e_u is the number of connected pairs of neighbors. The average clustering
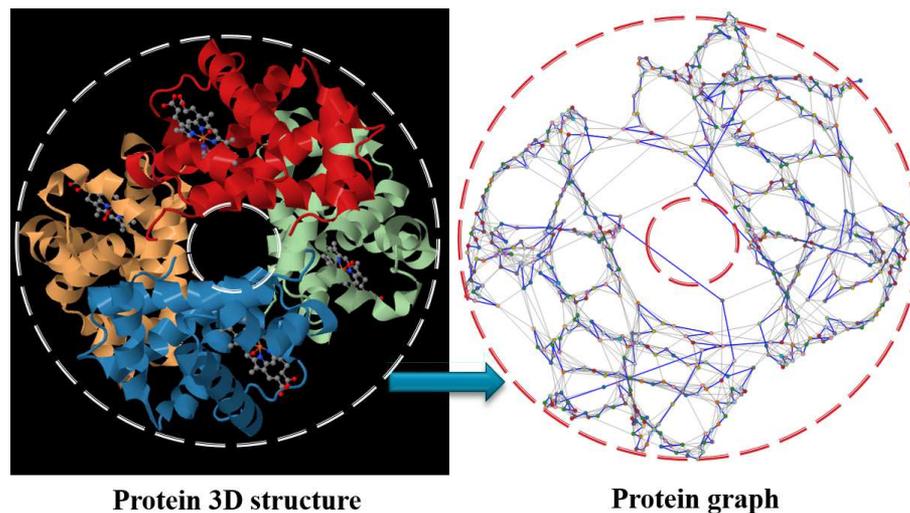
Fig. 1. The human hemoglobin protein 3D-structure (PDBID: 1GZX) and its corresponding graph representation. Nodes and edges represent, respectively, amino acids from the structure and links between them. Blue edges represent links from the primary structure and gray edges are spatial links between distant amino acids.

coefficient of a graph G, is given as the average value over all of its nodes. Formally: $C(G) = \frac{1}{|V|} \sum_{i=1}^{|V|} c(u_i)$.

A6- **Average effective eccentricity**: For a node u, the effective eccentricity represents the maximum length of the shortest paths between u and every other node v in G, $e(u) = max\{d(u,v) : v \in V, u \neq v\}$, where $d(u,v)$ is the length of the shortest path from u to v. The average effective eccentricity is defined as $Ae(G) = \frac{1}{|V|} \sum_{i=1}^{|V|} e(u_i)$.

A7- **Effective diameter**: It represents the maximum value of effective eccentricity over all nodes in the graph G, *i.e.*, $diam(G) = max\{e(u) \mid u \in V\}$ where $e(u)$ represents the effective eccentricity of u as defined above.

A8- **Effective radius**: It represents the minimum value of effective eccentricity over all nodes of G, $rad(G) = min\{e(u) \mid u \in V\}$.

A9- **Closeness centrality**: The closeness centrality measures how fast information spreads from a given node to other reachable nodes in the graph. For a node u, it represents the reciprocal of the average shortest path length between u and every other reachable node in the graph G, $C_c(u) = \frac{|V|-1}{\sum_{v \in \{V \setminus u\}} d(u,v)}$ where $d(u,v)$ is the length of the shortest path between the nodes u and v. For G, we consider the average value of closeness centrality of all its nodes, $C_c(G) = \frac{1}{|V|} \sum_{i=1}^{|V|} C_c(u_i)$.

A10- **Percentage of central nodes**: It is the ratio of the number of central nodes from the number of nodes in the graph. A node u is central if the value of its eccentricity is equal to the effective radius of the graph, $e(u) = rad(G)$.

A11- **Percentage of end points**: It represents the ratio of the number of nodes with $deg(u) = 1$ from the total number of nodes of G.

A12- **Number of distinct eigenvalues**: The adjacency matrix A of G has a set of eigenvalues. We count the number of distinct eigenvalues of A.

A13- **Spectral radius**: Let $\lambda_1, \lambda_2, ..., \lambda_m$ be the set of eigenvalues of the adjacency matrix A of G. The spectral radius of G, denoted $\rho(G)$, represents the largest magnitude eigenvalue, *i.e.*, $\rho(G) = max(|\lambda_i|)$ where $i \in \{1, .., m\}$.

A14- **Second largest eigenvalue**: The value of the second largest eigenvalue.

A15- **Energy**: The energy of an adjacency matrix A of a graph G is defined as the squared sum of the eigenvalues of A. Formally: $E(G) = \sum_{i=1}^{m} \lambda_i^2$.

A16- **Neighborhood impurity**: For a node u having a label $L(u)$ and a neighborhood $N(u)$, it is defined as $ImpDeg(u) = | L(v) : v \in N(u), L(u) \neq L(v) |$. The neighborhood impurity of G is the average $ImpDeg$ over all nodes.

A17- **Link impurity**: An edge $\{u,v\}$ is considered to be impure if $L(u) \neq L(v)$. The link impurity of a graph G with $|E|$ edges is defined as: $\frac{|\{u,v\} \in E : L(u) \neq L(v)|}{|E|}$.

A18- **Label entropy**: It measures the uncertainty of labels. For a graph G of k labels, it is defined as $E(G) = - \sum_{i=1}^{k} p(l_i) \log p(l_i)$, where l_i is the ith label.

2.3 ProtNN: Nearest Neighbor Protein Functional Classification

The general classification pipeline of ProtNN can be described as follows: first a preprocessing is performed on the reference protein database Ω in which a graph model G_P is created for each reference protein $P, \forall P \in \Omega$, according to Equation 1. A structural and topological description vector V_P is created for each graph model G_P, by computing the corresponding values of each of the structural and topological attributes described in Section 2.2.2. The resulting matrix $M_\Omega = \bigcup V_P, \forall P \in \Omega$, represents the preprocessed reference database that is used for prediction in ProtNN. In order to guarantee an equal participation of all used attributes in the classification, a min-max normalization ($x_{normalized} = \frac{x-min}{max-min}$, where x is an attribute value, min and max are the minimum and maximum values for the attribute vector) is applied on each attribute of M_Ω independently such that no attribute will dominate in the prediction. It is also worth mentioning that for real world applications M_Ω is only computed once, and can be incrementally updated with other attributes as well as newly added protein 3D-structures with no need to recompute the attributes for the entire set. This guarantees a high flexibility and easy extension of ProtNN in real world application. The prediction step in ProtNN is described in Algorithm 1. In prediction, a query protein 3D-structure Q with an unknown function, is first transformed into its corresponding graph model G_Q. The structural and topological attributes are computed for G_Q forming its query description vector V_Q. The query

protein Q is scanned against the entire reference database Ω, where the distance between V_Q and each of the reference vectors $\forall V_P \in M_\Omega$ is computed and stored in $Vdist_Q$, with respect to a distance measure. The k most similar reference proteins NN_Q^k are selected, and the query protein Q is predicted to exert the function with the highest number of votes across the set of NN_Q^k reference proteins, where k is a user-defined number of nearest neighbors.

Algorithm 1: ProtNN (The prediction step)

Data: Q: Query protein 3D-structure, M_Ω: Description matrix of the reference database of protein 3D-structures, k: number of similar

Result: C_Q: Functional class of Q

begin

  $G_Q \leftarrow$ create a graph model for Q according to Equation 1;

  $V_Q \leftarrow G_Q$ is embedded into a vector V using the attributes;

  $NN_Q^k \leftarrow \emptyset$;

  $Vdist_Q \leftarrow \emptyset$;

  foreach *(V_P in M_Ω)* **do**

    $Vdist_Q[P] \leftarrow$ distance(V_Q, V_P);   ▷ The distance between vectors of query protein Q and the reference protein P.

  $NN_Q^k \leftarrow Top_k(Vdist_Q)$; ▷ Select the k nearest reference protein neighbors

  $C_Q \leftarrow$ The functional class with the highest number of votes across the set of NN_Q^k reference proteins;

---

3 Experiments

3.1 Datasets

3.1.1 Benchmark Datasets

To assess the classification performance of ProtNN, we performed an experiment on six well-known benchmark datasets of protein structures that have previously been used in (Jin *et al.*, 2009, 2010; Fei and Huan, 2010; Zhu *et al.*, 2012). Each dataset is composed of positive protein examples that are from a selected protein family, and negative protein examples that are randomly sampled from the PDB (Berman *et al.*, 2000). Table 1 summarizes the characteristics of the six datasets. SCOP ID, Family name, Pos., and Neg. correspond respectively to the identifier of the protein family in SCOP (Andreeva *et al.*, 2008), its name, and the number of positive and negative examples. The selected positive protein families are Vertebrate phospholipase A2, G-protein family, C1-set domains, C-type lectin domains, and protein kinases, catalytic subunits.

Vertebrate phospholipase A2: Phospholipase A2 are enzymes from the class of hydrolase, which release the fatty acid from the hydroxyl of the carbon 2 of glycerol to give a phosphoglyceride lysophospholipid. They are located in most mammalian tissues.

G-proteins: G-proteins are also known as guanine nucleotide-binding proteins. These proteins are mainly involved in transmitting chemical signals originating from outside a cell into the inside of it. G-proteins are able to activate a cascade of further signaling events resulting a change in cell functions. They regulate metabolic enzymes, ion channels, transporter, and other parts of the cell machinery, controlling transcription, motility, contractility, and secretion, which in turn regulate diverse systemic functions such as embryonic development, learning and memory, and homeostasis.

C1-set domains: The C1-set domains are immunoglobulin-like domains, similar in structure and sequence. They resemble the antibody constant domains. They are mostly found in molecules involved in the

Table 1. Characteristics of the experimental datasets. SCOP ID: identifier of protein family in SCOP, Pos.: number of positive examples, Neg.: number of negative examples.

Dataset	SCOP ID	Family name	Pos.	Neg.
DS1	48623	Vertebrate phospholipase A2	29	29
DS2	52592	G-proteins	33	33
DS3	48942	C1-set domains	38	38
DS4	56437	C-type lectin domains	38	38
DS5	56251	Proteasome subunits	35	35
DS6	88854	Protein kinases, catalyc subunits	41	41

immune system, in the major histocompatibility complex class I and II complex molecules, and in various T-cell receptors.

C-type lectin domains: Lectins occur in plants, animals, bacteria and viruses. The C-type (Calcium-dependent) lectins are a family of lectins which share structural homology in their high-affinity carbohydrate-recognition domains. This dataset involves groups of proteins playing divers functions including cell-cell adhesion, immune response to pathogens and apoptosis.

Proteasome subunits: Proteasomes are critical protein complexes that primarily function to breakdown unneeded or damaged proteins. They are located in the nucleus and cytoplasm. The proteasome recycles damaged and misfolded proteins as well as degrades short-lived regulatory proteins. As such, it is a critical regulator of many cellular processes, including the cell cycle, DNA repair, signal transduction, and the immune response.

Protein kinases, catalyc subunits: Protein kinases, catalytic subunit play a role in various cellular processes, including division, proliferation, apoptosis, and differentiation. They are mainly proteins that modify other ones by chemically adding phosphate groups to them. This usually results in a functional change of the target protein by changing enzyme activity, cellular location, or association with other proteins. The catalytic subunits of protein kinases are highly conserved, and several structures have been solved, leading to large screens to develop kinase-specific inhibitors for the treatments of a number of diseases.

3.1.2 The Protein Data Bank

In order to assess the scalability of ProtNN to large scale real-world applications, we evaluate the runtime of our approach on the entire Protein Data Bank (PDB) (Berman *et al.*, 2000) which contains the updated list of all known protein 3D-structures. We use 94126 structure representing all the available protein 3D-structures in the PDB by the end of July 2014.

3.2 Protocol and Settings

Experiments were conducted on a *CentOS* Linux workstation with an Intel core-i7 CPU at 3.40 GHz, and 16.00 GB of RAM. All the experiments are performed in a single process mode with no parallelization. To transform protein into graph, we used a δ value of 7. The evaluation measure is the classification accuracy, and the evaluation technique is Leave-One-Out (LOO) where each dataset is used to create N classification scenarios, where N is the number of proteins in the dataset. In each scenario, a reference protein is used as a query instance and the rest of the dataset is used as reference. The aim is to correctly predict the class of the query protein. The classification accuracy for each dataset is averaged over results of all the N evaluations.
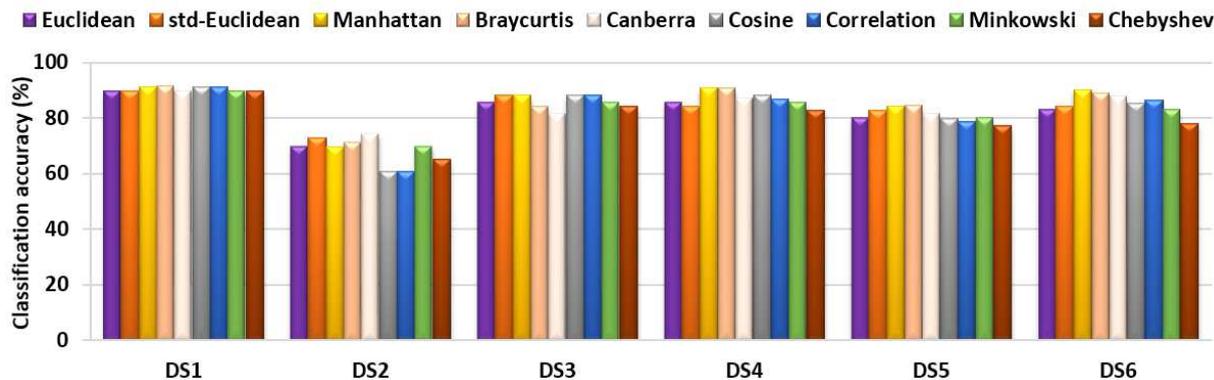
Fig. 2. Classification accuracy of ProtNN using different distance measures (k=1).

4 Results and Discussion

4.1 ProtNN Classification Results

4.1.1 Results Using Different Distance Measures

The classification algorithm of ProtNN supports any user-defined distance measure. In this section, we study the effect of varying the distance measure on the classification accuracy of ProtNN. We fixed k=1, and we used nine different well-known distance measures namely *Euclidean*, *standardized Euclidean* (std-euclidean), *Cosine*, *Manhattan*, *Correlation*, *Minkovski*, *Chebyshev*, *Canberra*, and *Braycurtis*. See (Sergio J. Rojas G., 2015) for a formal definition of these measures. Figure 2 shows the obtained results.

Overall, varying the distance measure did not significantly affect the classification accuracy of ProtNN on the six datasets. Indeed, the standard deviation of the classification accuracy of ProtNN with each distance measure did not exceed 3% on the six datasets. A ranking based on the average classification accuracy over the six datasets suggests the following descending order: (1) Manhattan, (2) Braycurtis, (3) std-Euclidean, (4) Canberra, (5) Cosine, (6) Euclidean - Minkowski, (8) Correlation, (9) Chebyshev.

4.1.2 Results Using Different Numbers of Nearest Neighbors

In the following, we evaluate the classification accuracy of ProtNN on each of the six benchmark datasets using different numbers of nearest neighbors $k \in [1,10]$. The same experiment is performed using each of the top-five distance measures. For simplicity, we only plot the average value of classification accuracy for each value of $k \in [1,10]$ over the six datasets using each of the top-five measures. Note that the standard deviation of the classification accuracy with each value of k did not exceed 2%. Figure 3 shows the obtained results. The number of nearest neighbors k has a clear effect on the accuracy of ProtNN. The results suggest that the "optimal" value of $k \in \{1,2\}$. The overall accuracy tendency shows that it decreases with higher values of k. This is due to the structural similarity that a query protein may share with other evolutionary close proteins exerting different functions. High values of k engender considering too many neighbors which may causes a misclassification.

4.1.3 Analysis of the Used Attributes

In the following, we study the importance of the used attributes in order to identify the most informative ones. We follow the Recursive Feature Elimination (RFE) (Guyon *et al.*, 2002) using ProtNN as the classifier. In RFE, one feature is removed at each iteration, where the remaining features are the ones that best enhance the classification accuracy. The pruning stops when no further enhancement is observed or no more features are left. The remaining features constitute the optimal subset for that context. In Table
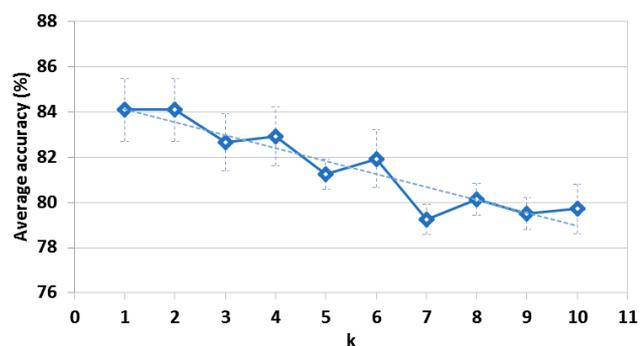

Fig. 3. Tendancy of the average accuracy of ProtNN for each value of $k \in [1,10]$ over the six datasets and using each of the top-five distance measures. The dashed line represents the linear tendancy of the results.

2, we record the ranking of the used attributes in our experiments. For more generalization, RFE was performed on each of the six datasets using a combination of each of the top-five distance measures and each of the top-five values of k. The total number of RFE experiments is 150. For each attribute, we count the total number of times it appeared in the optimal subset of attributes. A score of $\frac{total\ count}{number\ of\ experiments}$ is assigned to each attribute according to its total count. It is clear that the best subset of attributes is dataset dependent. The five most informative attributes are respectively: A15 (energy), A17 (link impurity), A12 (number of distinct eigenvalues), A16 (neighborhood impurity), and A13 (spectral radius). All spectral attributes showed to be very informative. Indeed, three of them (A15, A12, and A13) ranked in the top-five, and A14 (second largest eigenvalue) ranked in the top-ten (9th) with a score of 0.52 meaning that for more than half of all the experiments, all spectral attributes were selected in the optimal subset of attributes. Unsurprisingly, A11 (percentage of end points) ranked last with a very low score. This is because proteins are dense molecules and thus very few nodes of their respective graphs will be end points (extremity amino acids in the primary structure with no spatial links). Label attributes also showed to be very informative. Indeed, A17, A16, and A18 (label entropy) ranked respectively 2nd, 4th, and 6th with scores of more than 0.61. This is due to the importance of the distribution of the types of amino acids and their interactions. Both have to follow a certain harmony in the structure in order to exert a particular function. A9 (closeness centrality), A5 (average clustering coefficient) and A8 (effective radius) ranked in the top-ten with scores of more than 0.5 (A8 scored 0.49 $\simeq$ 0.5). However, all A1 (number of nodes), A2 (number of edges), A3

Table 2. Empirical ranking of the structural and topological attributes.

Data	Attributes																	
	A1	A2	A3	A4	A5	A6	A7	A8	A9	A10	A11	A12	A13	A14	A15	A16	A17	A18
DS1	0	2	1	6	2	1	5	9	10	1	2	8	6	13	16	17	12	17
DS2	8	12	15	16	18	4	9	16	23	17	9	21	11	14	25	17	23	9
DS3	8	13	2	6	17	10	16	11	11	4	8	18	21	2	21	23	9	18
DS4	4	7	21	17	20	6	11	17	16	7	2	14	21	22	20	21	24	17
DS5	12	12	8	10	12	5	7	7	17	17	7	23	23	9	20	9	19	18
DS6	5	11	9	8	11	6	14	14	13	6	1	17	14	18	24	10	17	13
Total	37	57	56	63	80	32	62	74	90	52	29	**101**	96	78	**126**	97	**104**	92
Score	0.25	0.38	0.37	0.42	0.53	0.21	0.41	0.49	0.6	0.35	0.19	**0.67**	**0.64**	0.52	**0.84**	**0.65**	**0.69**	0.61
Rank	16	13	14	11	8	17	12	10	7	15	18	**3**	**5**	9	**1**	**4**	**2**	6

(average degree), A4 (density), A6 (average effective eccentricity), A7 (effective diameter), and A10 (percentage of central nodes) scored less than 0.5. This is because each one of them is represented by one of the top-ten attributes and thus presents a redundant information. A6 and A9 are both expressed based on all shortest paths of the graph. Both A7 and A8 are expressed based on A6. A10 is expressed based on A8 and thus on A6 too. A1, A2, A3, and A4 are all highly correlated to A5.

4.1.4 Comparison with Other Classification Techniques

We compare our approach with multiple state-of-the-art approaches for protein function prediction namely: sequence alignment-based classification (using Blast (Altschul *et al.*, 1990)), structural alignment-based classification (using Combinatorial Extension (CE) (Shindyalov and Bourne, 1998), Sheba (Jung and Lee, 2000), and FatCat (Ye and Godzik, 2003)), and substructure(subgraph)-based classification (using GAIA (Jin *et al.*, 2010), LPGBCMP (Fei and Huan, 2010), and D&D (Zhu *et al.*, 2012)). For sequence and structural alignment-based classification, we align each protein against all the rest of the dataset. We assign to the query protein the function of the reference protein with the best hit score. For the substructure-based approaches, all the selected approaches are mainly for mining discriminative subgraphs. LPGBCMP is used with max_{var} = 1 and d = 0.25 for, respectively, feature consistency map building and overlapping. In (Fei and Huan, 2010), LPGBCMP outperformed several other approaches from the literature including LEAP (Yan *et al.*, 2008), gPLS (Saigo *et al.*, 2008), and COM (Jin *et al.*, 2009) on the classification of the same six benchmark datasets. GAIA showed in (Jin *et al.*, 2010) that it outperformed other state-of-the-art approaches namely COM and graphSig (Ranu and Singh, 2009). D&D have showed in (Zhu *et al.*, 2012) that it also outperformed COM and graphSig, and that it is highly competitive to GAIA. For all these approaches, the discovered substructures are considered as features for describing each example of the original data. The constructed description matrix is used for training in the classification. For our approach, we show the classification accuracy results of ProtNN with RFE using std-Euclidean distance. We also show the best results of ProtNN (denoted ProtNN*) with RFE using each of the top-five distance measures. We use k = 1 both for ProtNN and ProtNN*. Table 3 shows the obtained results.

The alignment-based approaches FatCat and Sheba outperformed CE, Blast, and all the subgraph-based approaches. Indeed, FatCat scored best with three of the first four datasets and Sheba scored best with the two last datasets. Except CE, all the other approaches scored on average better than Blast. This shows that the spatial information constitutes an important asset for functional classification by emphasizing structural properties that the primary sequence alone do not provide. For the subgraph-based approaches, D&D scored better than LPGBCMP and GAIA on all cases

except with DS1 where GAIA scored best. On average, ProtNN* ranked first with the smallest distance between its results and the best obtained accuracies with each dataset. This is because ProtNN considers both structural information, and hidden topological properties that are omitted by the other approaches.

4.2 Scalability and Runtime Analysis

Besides being accurate, an efficient approach for functional classification of protein 3D-structures has to be very fast in order to provide practical usage that meets the increasing load of data in real-world applications. In this section, we study the runtime of ProtNN and FatCat, the most competitive approach in our previous comparative experiments. We analyze the variation of runtime for both approaches with higher numbers of proteins ranging from 10 to 100 3D-structures with a step-size of 10. In Figure 4, we report the runtime results in $\log_{10}$-scale. A huge gap is clearly observed between the runtime of ProtNN and that of FatCat. The gap gets larger with higher numbers of proteins. Indeed, FatCat took over 5570 seconds with the 100 proteins while ProtNN (all) did not exceed 118 seconds for the same set which means that our approach is 47x faster than FatCat on that experiment. The average runtime of graph transformation of ProtNN was 0.8 second and that of the computation of attributes was 0.6 second for each protein. The total runtime of similarity search and function prediction of ProtNN was only 0.1 on the set of 100 proteins. Note that in real-world applications, the preprocessing (graph transformation and attribute computation) of the reference database is performed only once and the latter can be updated with no need to recompute the existing values. This ensures computational efficiency and easy extension of our approach.

4.2.1 Scalability to a PDB-wide classification

We further evaluate the scalability of ProtNN in the classification of the entire Protein Data Bank (described in 3.1.2). We also show the runtime for FatCat and CE (the structural alignment approaches used in the PDB website[1]). We recall that the experiments are on a single process mode with no parallelization for all the approaches. Note that in the PDB website, the structural alignment is whether pre-computed for structures of the database, or only performed on a sub-sample of the PDB for customized or local files. Table 4 shows the obtained results. It is clear that the computation of attributes is the most expensive part of our approach as some attributes are very complex. However, building the graph models and the computation of attributes represent the preprocessing step and are only performed once for the reference database. The classification step took almost three hours with an average runtime of 0.1 second for the classification of each protein against the entire PDB. All and all ProtNN

---

[1] http://www.rcsb.org/pdb/

Table 3. Accuracy comparison of ProtNN with other classification techniques.

Dataset	Classification approach								
	Blast	**Sheba**	**FatCat**	**CE**	**LPGBCMP**	**D&D**	**GAIA**	**ProtNN**	**ProtNN***
DS1	0.88	0.81	**1**	0.45	0.88	0.93	**1**	0.97	0.97
DS2	0.82	0.86	**0.89**	0.49	0.73	0.76	0.66	0.8	**0.89**
DS3	0.9	0.95	0.84	0.59	0.90	0.96	0.89	0.96	**0.97**
DS4	0.76	0.92	**1**	0.46	0.9	0.93	0.89	0.97	0.97
DS5	0.86	**0.99**	0.94	0.76	0.87	0.89	0.72	0.9	0.94
DS6	0.78	**1**	0.94	0.81	0.91	0.91	0.95	0.96	0.96
Avg. accuracy[1]	0.83±0.05	0.92±0.07	0.94±0.06	0.59±0.15	0.86±0.06	0.9±0.07	0.84±0.12	0.93±0.06	**0.95±0.03**
Avg. distances[2]	0.14±0.07	0.05±0.07	0.04±0.05	0.38±0.15	0.11±0.03	0.7±0.04	0.14±0.09	0.05±0.03	**0.02±0.01**
Rank	8	4	2	9	6	5	7	3	**1**

[1] Average classification accuracy of each classification approach over the six datasets.

[2] Average of the distances between the accuracy of each approach and the best obtained accuracy with each dataset.
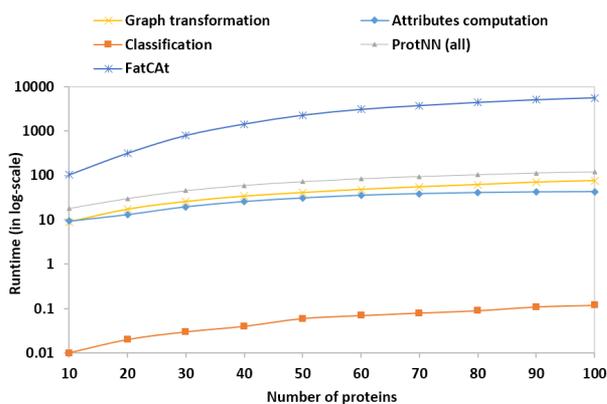

Fig. 4. Runtime comparison in log-scale of ProtNN and FatCat. The running time of ProtNN is separated for the main steps.

Table 4. Runtime results of ProtNN, FatCat and CE on the entire Protein Data Bank.

Task	Total runtime[1]	Runtime[1]/protein
Building graph models	23h:9m:57s	0.9s
Computation of attributes	5d:8h:12m:29s	4.9s
Classification	2h:55m:15s	0.1s
ProtNN (all)	6d:10h:17m:41s	5.9s
FatCat	Forever[2]	1d:18h:31m:35s[3]
CE	Forever[2]	1d:8h:37m:34s[3]

[1] The runtime is expressed in terms of days:hours:minutes:seconds

[2] The program did not finish running within two weeks

[3] The average runtime of randomly selected 100 proteins

runtime was less than a week with an average runtime of 5.9 seconds for the preprocessing and classification of each protein 3D-structure against the entire PDB. On the other hand, both FatCat and CE did not finish running within two weeks. We computed the average runtime for each approach on the classification of a sample of 100 proteins against all the PDB. On average FatCat and CE took respectively more than 42 and 32 hours per protein making our approach faster than both approaches with thousands orders of magnitude on the classification of a 3D-structure against the entire PDB.

5 Conclusion

In this paper, we proposed ProtNN, a new fast and accurate approach for protein function prediction. We defined a graph transformation and embedding model that incorporates explicit as well as hidden structural and topological properties of the 3D-structure of proteins. We successfully implemented the proposed model and we experimentally demonstrated that it allows to detect similarity and to predict the function of protein 3D-structures efficiently. Empirical results of our experiments showed that considering structural information constitutes a major asset for accurately identifying protein functions. They also showed that the alignment-based classification as well as subgraph-based classification present very competitive approaches. Yet, as the number of pairwise comparisons between proteins grows tremendously with the size of dataset, enormous computational costs would be the results of more detailed models. Here we highlight that ProtNN could accurately classify multiple benchmark datasets from the literature with very low computational costs. With all large-scale studies, it is an asset that ProtNN scale up to a PDB-wide dataset in a single-process mode with no parallelization, where it outperformed state-of-the-art approaches with thousands order of magnitude in runtime on classifying a 3D-structure against the entire PDB. In future works, we aim to integrate more proven protein functional attributes in our model to further enhance the accuracy of the prediction system.

Acknowledgements

References

Altschul, S., Gish, W., Miller, W., Myers, E., and Lipman, D. (1990). Basic local alignment search tool. *Journal of Molecular Biology*, **215**, 403–410.

Andreeva, A., Howorth, D., Chandonia, J.-M., Brenner, S. E., Hubbard, T. J. P., Chothia, C., and Murzin, A. G. (2008). Data growth and its impact on the scop database: new developments. *Nucleic Acids Research*, **36**(1), D419–D425.

Berman, H. M., Westbrook, J. D., Feng, Z., Gilliland, G., Bhat, T. N., Weissig, H., Shindyalov, I. N., and Bourne, P. E. (2000). The protein

data bank. *Nucleic Acids Research*, **28**(1), 235–242.

Borgwardt, K. M., Ong, C. S., Schönauer, S., Vishwanathan, S. V. N., Smola, A. J., and Kriegel, H. (2005). Protein function prediction via graph kernels. In *Proceedings Thirteenth International Conference on Intelligent Systems for Molecular Biology 2005, Detroit, MI, USA, 25-29 June 2005*, pages 47–56.

Brenner, S. E. and Levitt, M. (2000). Expectations from structural genomics. *Protein Sci*, **9**.

Budowski-Tal, I., Nov, Y., and Kolodny, R. (2010). Fragbag, an accurate representation of protein structure, retrieves structural neighbors from the entire pdb quickly and accurately. *Proceedings of the National Academy of Sciences*, **107**(8), 3481–3486.

Dhifli, W., Saidi, R., and Mephu Nguifo, E. (2014). Smoothing 3D protein structure motifs through graph mining and amino-acids similarities. *Journal of Computational Biology*, **21**(2), 162–172.

Fei, H. and Huan, J. (2010). Boosting with structure information in the functional space: an application to graph classification. In *ACM knowledge discovery and data mining conference (KDD)*, pages 643–652.

Gibert, J., Valveny, E., and Bunke, H. (2010). Graph of words embedding for molecular structure-activity relationship analysis. In *Progress in Pattern Recognition, Image Analysis, Computer Vision, and Applications*, volume 6419 of *Lecture Notes in Computer Science*, pages 30–37. Springer Berlin Heidelberg.

Guyon, I., Weston, J., Barnhill, S., and Vapnik, V. (2002). Gene selection for cancer classification using support vector machines. *Machine Learning*, **46**(1-3), 389–422.

Jin, N., Young, C., and Wang, W. (2009). Graph classification based on pattern co-occurrence. In *ACM International Conference on Information and Knowledge Management*, pages 573–582.

Jin, N., Young, C., and Wang, W. (2010). GAIA: graph classification using evolutionary computation. In *Proceedings of the 2010 ACM SIGMOD International Conference on Management of data*, pages 879–890. ACM.

Jung, J. and Lee, B. (2000). Protein structure alignment using environmental profiles. *Protein Engineering*, **13**, 535–543.

Lee, D., Redfern, O., and Orengo, C. (2007). Predicting protein function from sequence and structure. *Nat Rev Mol Cell Biol*, **8**.

Leskovec, J., Kleinberg, J., and Faloutsos, C. (2005). Graphs over time: densification laws, shrinking diameters and possible explanations. In *eleventh ACM SIGKDD international conference on Knowledge discovery in data mining*, pages 177–187. ACM.

Li, G., Semerci, M., Yener, B., and Zaki, M. J. (2012). Effective graph classification based on topological and label attributes. *Statistical Analysis and Data Mining*, **5**(4), 265–283.

Meysman, P., Zhou, C., Cule, B., Goethals, B., and Laukens, K. (2015). Mining the entire protein databank for frequent spatially cohesive amino acid patterns. *BioData Mining*, **8**, 4.

Molloy, K., Van, M. J., Barbara, D., and Shehu, A. (2014). Exploring representations of protein structure for automated remote homology detection and mapping of protein structure space. *BMC Bioinformatics*, **15**(8), 1–14.

Ranu, S. and Singh, A. K. (2009). Graphsig: A scalable approach to mining significant subgraphs in large graph databases. In *IEEE 25th International Conference on Data Engineering.*, pages 844–855.

Saigo, H., Krämer, N., and Tsuda, K. (2008). Partial least squares regression for graph mining. In *ACM knowledge discovery and data mining conference (KDD)*, pages 578–586.

Sergio J. Rojas G., Erik A Christensen, F. J. B.-S. (2015). *Learning SciPy for Numerical and Scientific Computing - Second Edition*. Community experience distilled. Packt Publishing.

Shindyalov, I. N. and Bourne, P. E. (1998). Protein structure alignment by incremental combinatorial extension of the optimum path. *Protein Engineering*, **11**(9), 739–747.

Sillitoe, I., Lewis, T. E., Cuff, A. L., Das, S., Ashford, P., Dawson, N. L., Furnham, N., Laskowski, R. A., Lee, D., Lees, J. G., Lehtinen, S., Studer, R. A., Thornton, J. M., and Orengo, C. A. (2015). CATH: comprehensive structural and functional annotations for genome sequences. *Nucleic Acids Research*, **43**(Database-Issue), 376–381.

Wolpert, D. and Macready, W. G. (1997). No free lunch theorems for optimization. *IEEE Transactions on Evolutionary Computation*, **1**(1), 67–82.

Yan, X., Cheng, H., Han, J., and Yu, P. S. (2008). Mining significant graph patterns by leap search. In *Proceedings of the ACM SIGMOD international conference on Management of data*, SIGMOD, pages 433–444. ACM.

Ye, Y. and Godzik, A. (2003). Flexible structure alignment by chaining aligned fragment pairs allowing twists. *Bioinformatics*, **19**, 246–255.

Zhu, Y., Yu, J. X., Cheng, H., and Qin, L. (2012). Graph classification: a diversified discriminative feature selection approach. In *21st ACM International Conference on Information and Knowledge Management*, pages 205–214. ACM.